

# QCD evolution of the Sivers asymmetry

Miguel G. Echevarria,<sup>1,\*</sup> Ahmad Idilbi,<sup>2,†</sup> Zhong-Bo Kang,<sup>3,‡</sup> and Ivan Vitev<sup>3,§</sup>

<sup>1</sup>*Nikhef Theory Group, Science Park 105, 1098 XG Amsterdam, The Netherlands*

<sup>2</sup>*Department of Physics, Pennsylvania State University, University Park, PA 16802, USA*

<sup>3</sup>*Theoretical Division, Los Alamos National Laboratory, Los Alamos, NM 87545, USA*

(Dated: April 8, 2014)

We study the QCD evolution of the Sivers effect in both semi-inclusive deep inelastic scattering (SIDIS) and Drell-Yan production (DY). We pay close attention to the non-perturbative spin-independent Sudakov factor in the evolution formalism and find a universal form which can describe reasonably well the experimental data on the transverse momentum distributions in SIDIS, DY lepton pair and  $W/Z$  production. With this Sudakov factor at hand, we perform a global fitting of all the experimental data on the Sivers asymmetry in SIDIS from HERMES, COMPASS and Jefferson Lab. We then make predictions for the Sivers asymmetry in DY lepton pair and  $W$  production that can be compared to the future experimental measurements to test the sign change of the Sivers functions between SIDIS and DY processes and constrain the sea quark Sivers functions.

## I. INTRODUCTION

In recent years, transverse spin physics has become one of the most active areas of high energy hadron physics research. In particular, the experimental study and theoretical understanding of single transverse spin asymmetries has resulted in a much deeper understanding of the nucleon structure [1–5]. It has been realized that these observables can provide information on the parton’s intrinsic transverse motion, which presents a path to three-dimensional proton tomography. The information about the three-dimensional proton structure is encoded in the so-called transverse momentum dependent distribution functions (TMDs), which provide a new domain to study the strong interaction dynamics. They also open a new window to study the validity of QCD factorization theorems and the universality of the associated TMD parton distribution functions (TMDPDFs) and/or fragmentation functions (TMDFFs) [6–14].

One of the most studied asymmetries has been the Sivers effect. It originates from a special TMD called the Sivers function [15], which represents a distribution of unpolarized partons inside a transversely polarized proton through a correlation between the parton’s transverse momentum and the proton polarization vector. The Sivers effect has gathered a lot of attention largely because of its unique property: the Sivers function is not exactly universal, instead, it exhibits time-reversal modified universality [6–8, 10, 16]. Based on parity and time-reversal invariance of QCD, it was shown that the quark Sivers function in semi-inclusive deep inelastic scattering (SIDIS) and those in the Drell-Yan (DY) process are equal in magnitude and opposite in sign to each other. This sign change of the Sivers functions between SIDIS and DY is one of the most important predictions in the transverse spin physics and provides a critical test of the QCD factorization formalism and our understanding of spin asymmetries.

The Sivers asymmetry has been measured in the SIDIS process by HERMES [17], COMPASS [18, 19], and Jefferson Lab (JLab) [20] experiments. Future measurements of the Sivers asymmetry in DY production have been planned [4, 21–24] to verify the expected sign change. In anticipation of these new results, we need reliable predictions for the Sivers asymmetry in different processes. It is important to keep in mind that the Sivers asymmetry was measured in SIDIS for typical momentum scales  $Q \sim 1–3$  GeV, while for the DY-type processes it will be measured at much larger momentum scales  $Q \sim 4–90$  GeV. Any reliable predictions will certainly have to include a correct understanding of the  $Q$ -dependence of the Sivers asymmetry. In other words, we have to properly include its energy evolution [25–30].

QCD evolution equations for the TMDs have been derived using different approaches [26–29], and they are consistent with each other *perturbatively*. For QCD evolution equations of the associated spin-dependent collinear PDFs and/or FFs, see Refs. [31–38]. One of the difficulties related to the QCD evolution of TMDs lies in the fact that the complete evolution formalism contains both perturbative and non-perturbative parts [39–44]. Because of this, the evolved asymmetries in phenomenological applications can be quite different depending on the treatment of the non-perturbative part [45–48] even though the perturbative evolution kernel is exactly the same. The non-perturbative part should be universal and extracted from the experimental data and in this paper we pay close attention to its role in the evolution kernel. Thus, we first concentrate on the spin-averaged differential cross section, which can be used

\* m.g.echevarria@nikhef.nl

† aui13@psu.edu

‡ zkang@lanl.gov

§ ivitev@lanl.gov

to constrain the non-perturbative Sudakov factor. Since one of the essential parts of the Sudakov factor is universal and spin-independent, its reliable extraction from spin-averaged cross sections will result in an improved analysis of the Sivers asymmetries in the transverse spin-dependent scatterings. With this new Sudakov factor, we then perform a global fitting of the HERMES, COMPASS and JLab experimental data on polarized reactions to extract the Sivers functions. Finally, we reverse the sign of the quark Sivers functions to make predictions for the DY dilepton and  $W$  boson production that will be measured in the near future to test the sign change of the Sivers effect.

## II. QCD EVOLUTION OF TMDs: UNPOLARIZED DIFFERENTIAL CROSS SECTIONS

In this section, we review the QCD evolution of TMDs [26–29]. We propose a simple non-perturbative Sudakov factor in the evolution formalism and demonstrate that it leads to a reasonably good description of the transverse momentum distribution for hadron production in SIDIS, as well as DY dilepton and  $W/Z$  boson production in  $pp$  collisions. We present a detailed comparison of our results with the experimental data on the hadron multiplicity distributions in SIDIS from both HERMES and COMPASS experiments, DY dilepton production at Fermilab fixed-target experiments and  $W/Z$  boson production at the Tevatron and LHC energies.

### A. QCD evolution of TMDs

Our main focus is the transverse momentum dependent distribution function  $F(x, k_\perp; Q)$  [26, 49]<sup>1</sup>, which is probed at a momentum scale  $Q$  and carries the collinear momentum fraction  $x$  and a transverse component  $k_\perp$ . Since the evolution formalism is simpler in the coordinate space, we define the Fourier transform of  $F(x, k_\perp; Q)$  in the two-dimensional coordinate space (referred to as  $b$ -space below) as

$$F(x, b; Q) = \int d^2 k_\perp e^{-ik_\perp \cdot b} F(x, k_\perp; Q). \quad (1)$$

The energy evolution of the TMD  $F(x, b; Q)$  in the  $b$ -space has been derived by various groups and has the following form [26–29]:

$$F(x, b; Q_f) = F(x, b; Q_i) \exp \left\{ - \int_{Q_i}^{Q_f} \frac{d\mu}{\mu} \left( \Gamma_{\text{cusp}} \ln \frac{Q_f^2}{\mu^2} + \gamma^V \right) \right\} \left( \frac{Q_f^2}{Q_i^2} \right)^{-D(b; Q_i)}, \quad \frac{dD}{d \ln \mu} = \Gamma_{\text{cusp}}, \quad (2)$$

Here  $\Gamma_{\text{cusp}}$  stands for the well-known cusp anomalous dimension with non cusp  $\gamma^V$  [29],  $Q_i$  and  $Q_f$  are the initial and final momentum scales for the QCD evolution, respectively. It is important to emphasize that the evolution kernel in the right hand side of Eq. (2) is valid only in the perturbative region, i.e., when  $1/b \gg \Lambda_{\text{QCD}}$ .

The function  $F(x, b; Q)$  can represent any TMD. The relevant ones for this paper will be the unpolarized transverse momentum dependent PDFs and FFs, and the  $k_\perp$ -weighted Sivers function. They are defined as follows:

$$f_{q/A}(x, b; Q) = \int d^2 k_\perp e^{-ik_\perp \cdot b} f_{q/A}(x, k_\perp^2; Q), \quad (3)$$

$$D_{h/q}(z, b; Q) = \frac{1}{z^2} \int d^2 p_T e^{-ip_T \cdot b/z} D_{h/q}(z, p_T^2; Q), \quad (4)$$

$$f_{1T}^{\perp q(\alpha)}(x, b; Q) = \frac{1}{M} \int d^2 k_\perp e^{-ik_\perp \cdot b} k_\perp^\alpha f_{1T}^{\perp q}(x, k_\perp^2; Q), \quad (5)$$

where  $f_{q/A}(x, k_\perp^2; Q)$  and  $D_{h/q}(z, p_T^2; Q)$  are the unpolarized transverse momentum dependent PDF and FF in momentum space, while  $f_{1T}^{\perp q}(x, k_\perp^2; Q)$  is the quark Sivers function in the so-called Trento convention [52]. It is important to keep in mind that  $f_{q/A}(x, b; Q)$ ,  $D_{h/q}(z, b; Q)$ , and  $f_{1T}^{\perp q(\alpha)}(x, b; Q)$  follow exactly the same QCD evolution in the perturbative region as in Eq. (2) [25, 28, 29, 50].

---

<sup>1</sup> The properly defined TMDs depend on two scales [26–29], i.e., the factorization scale  $\mu$  and another scale  $\zeta$  related to the relevant high scale in the considered process, say the virtuality  $Q$  of the photon in SIDIS process. We set them equal for simplicity,  $\mu = \sqrt{\zeta} = Q$ .

In this paper we apply the well-known Collins-Soper-Sterman (CSS) approach [39–41] and choose an initial scale  $Q_i = c/b$  to start the evolution of the TMDs. Here  $c = 2e^{-\gamma_E}$ , with  $\gamma_E \approx 0.577$  the Euler's constant. Thus, the evolution of a TMD from an initial scale  $Q_i = c/b$  up to the scale  $Q_f = Q$  is given by

$$F(x, b; Q) = F(x, b; c/b) \exp \left\{ - \int_{c/b}^Q \frac{d\mu}{\mu} \left( A \ln \frac{Q^2}{\mu^2} + B \right) \right\} \left( \frac{Q^2}{(c/b)^2} \right)^{-D(b; c/b)}, \quad (6)$$

which we have written in terms of the conventional CSS notations with functions  $A$  and  $B$ :  $A = \Gamma_{\text{cusp}}$  and  $B = \gamma^V$  in Eq. (2). These functions, together with the  $D$  term, are perturbatively expanded as in  $A = \sum_{n=1}^{\infty} A^{(n)} (\alpha_s/\pi)^n$ ,  $B = \sum_{n=1}^{\infty} B^{(n)} (\alpha_s/\pi)^n$  and  $D = \sum_{n=1}^{\infty} D^{(n)} (\alpha_s/\pi)^n$ . The coefficients we keep in our phenomenological analysis, which corresponds to next-to-leading-logarithmic (NLL) accuracy [29], are given by [25, 27, 29, 39–41]:

$$A^{(1)} = C_F, \quad (7)$$

$$A^{(2)} = \frac{C_F}{2} \left[ C_A \left( \frac{67}{18} - \frac{\pi^2}{6} \right) - \frac{10}{9} T_{Rn_f} \right], \quad (8)$$

$$B^{(1)} = -\frac{3}{2} C_F, \quad (9)$$

$$D^{(1)} = \frac{C_F}{2} \ln \frac{Q_i^2 b^2}{c^2} \quad \longrightarrow \quad D^{(1)}(b; Q_i = c/b) = 0. \quad (10)$$

In the region where  $1/b \gg \Lambda_{\text{QCD}}$  we can expand the initial TMD  $F(x, b; \mu = c/b)$  in terms of the corresponding collinear function as follows

$$F_{i/h}(x, b; \mu) = \sum_a \int_x^1 \frac{d\xi}{\xi} C_{i/a} \left( \frac{x}{\xi}, b; \mu \right) f_{a/h}(\xi, \mu) + \mathcal{O}(b \Lambda_{\text{QCD}}), \quad (11)$$

where  $C_{i/a}(z, b; \mu) = \sum_{n=0}^{\infty} C_{i/a}^{(n)} (\alpha_s/\pi)^n$  is the perturbatively calculable coefficient function with the leading order (LO) result  $C_{i/a}^{(0)} = \delta_{ia} \delta(1-z)$  [25, 39, 40, 43]. Consistently with the NLL accuracy, in our phenomenological studies we only keep the LO results for the coefficient functions. In other words,

$$f_{q/A}(x, b; \mu) = f_{q/A}(x, \mu) + \dots, \quad (12)$$

$$D_{h/q}(z, b; \mu) = \frac{1}{z^2} D_{h/q}(z, \mu) + \dots, \quad (13)$$

$$f_{1T, \text{SIDIS}}^{\perp q(\alpha)}(x, b; \mu) = \left( \frac{ib^\alpha}{2} \right) T_{q,F}(x, x, \mu) + \dots, \quad (14)$$

where “...” represents the contributions from higher order coefficients  $C_{i/a}^{(n)}$  with  $n \geq 1$  that are neglected in our current study. The functions  $f_{q/A}(x, \mu)$  and  $D_{h/q}(z, \mu)$  are the collinear PDFs and FFs, while  $T_{q,F}(x, x, \mu)$  is the twist-3 Qiu-Sterman quark-gluon correlation function. Eq. (14) was first derived in [25] and the result is not surprising because the Qiu-Sterman function is the first  $k_\perp$ -moment of the quark Sivers function [8, 10]. The subscript “SIDIS” on the left-hand side emphasizes that the equation is valid for the quark Sivers function measured in the SIDIS process. For the DY process there is an extra minus sign on the right-hand side.

With this in mind, we obtain the *perturbative* part (i.e., valid only when  $1/b \gg \Lambda_{\text{QCD}}$ ) of the TMD  $F(x, b; Q)$  at NLL as

$$F_{\text{pert}}(x, b; Q) = f(x, c/b) \exp \left\{ - \int_{c/b}^Q \frac{d\mu}{\mu} \left( A \ln \frac{Q^2}{\mu^2} + B \right) \right\}, \quad (15)$$

where  $f(x, c/b)$  is the corresponding collinear function at scale  $\mu = c/b$ . In order to Fourier transform back and obtain the corresponding TMD  $F(x, k_\perp; Q)$  in transverse momentum space,

$$F(x, k_\perp; Q) = \int \frac{d^2 b}{(2\pi)^2} e^{ik_\perp \cdot b} F(x, b; Q) = \frac{1}{2\pi} \int_0^\infty db b J_0(k_\perp b) F(x, b; Q), \quad (16)$$

with  $J_0$  being the Bessel function of the zeroth order, one needs the information for the whole  $b \in [0, \infty]$  region. Thus, to perform the Fourier transform, we have to extrapolate to the non-perturbative large- $b$  region. For this part, we follow the standard CSS approach [39, 41] and introduce a non-perturbative Sudakov factor  $R_{NP}(x, b, Q)$  as follows

$$F(x, b; Q) = F_{\text{pert}}(x, b_*; Q) R_{NP}(x, b, Q), \quad (17)$$

where  $b_* = b/\sqrt{1 + (b/b_{\max})^2}$  and  $b_{\max}$  is introduced such that  $b_* \approx b$  at small  $b \ll b_{\max}$  region, while it approaches the limit  $b_{\max}$  when  $b$  becomes non-perturbatively large. The value of  $b_{\max}$  is typically chosen to be of order  $\sim 1$  GeV $^{-1}$  and should be thought of as characterizing the boundary of the perturbative region of the  $b$ -dependence. The non-perturbative Sudakov factor  $R_{\text{NP}}(b, Q) = \exp(-S_{\text{NP}})$  has been extensively studied. It has been extracted from the experimental data, in particular from  $W/Z$  boson production at high energies [41, 51], and is mainly constrained by the large  $Q$  fits. In this work we want to find a universal form, such that it can be used to describe the experimental data for SIDIS at relatively low  $Q$ , DY dilepton production at intermediate  $Q$ , and  $W/Z$  boson production at large  $Q$ . A simple widely used non-perturbative Sudakov exponent  $S_{\text{NP}}$  has the following form [41, 51, 53, 54]

$$S_{\text{NP}}^{\text{pdf}}(b, Q) = b^2 \left( g_1^{\text{pdf}} + \frac{g_2}{2} \ln \frac{Q}{Q_0} \right), \quad (18)$$

$$S_{\text{NP}}^{\text{ff}}(b, Q) = b^2 \left( g_1^{\text{ff}} + \frac{g_2}{2} \ln \frac{Q}{Q_0} \right), \quad (19)$$

$$S_{\text{NP}}^{\text{sivers}}(b, Q) = b^2 \left( g_1^{\text{sivers}} + \frac{g_2}{2} \ln \frac{Q}{Q_0} \right), \quad (20)$$

for the unpolarized TMDPDFs, TMDFFs, and the weighted quark Sivers function as in Eqs. (3), (4), and (5), respectively. Combining the  $b_*$  prescription with Eqs. (15) and (17), we can write out the evolved TMDs explicitly as

$$f_{q/A}(x, b; Q) = f_{q/A}(x, c/b_*) \exp \left\{ - \int_{c/b_*}^Q \frac{d\mu}{\mu} \left( A \ln \frac{Q^2}{\mu^2} + B \right) \right\} \exp \left\{ -b^2 \left( g_1^{\text{pdf}} + \frac{g_2}{2} \ln \frac{Q}{Q_0} \right) \right\}, \quad (21)$$

$$D_{h/q}(z, b; Q) = \frac{1}{z^2} D_{h/q}(x, c/b_*) \exp \left\{ - \int_{c/b_*}^Q \frac{d\mu}{\mu} \left( A \ln \frac{Q^2}{\mu^2} + B \right) \right\} \exp \left\{ -b^2 \left( g_1^{\text{ff}} + \frac{g_2}{2} \ln \frac{Q}{Q_0} \right) \right\}, \quad (22)$$

$$f_{1T, \text{SIDIS}}^{\perp q(\alpha)}(x, b; Q) = \left( \frac{ib^\alpha}{2} \right) T_{q,F}(x, c/b_*) \exp \left\{ - \int_{c/b_*}^Q \frac{d\mu}{\mu} \left( A \ln \frac{Q^2}{\mu^2} + B \right) \right\} \exp \left\{ -b^2 \left( g_1^{\text{sivers}} + \frac{g_2}{2} \ln \frac{Q}{Q_0} \right) \right\}. \quad (23)$$

It is important to realize that  $g_2$  is universal for all different types of TMDs and is certainly spin-independent, which is one of the important predictions of QCD factorization theorems involving TMDs [26, 27]. On the other hand, the constant term  $g_1$  depends on the type of TMDs, and can be interpreted as the intrinsic transverse momentum width for the relevant TMDs at the momentum scale  $Q_0$  [27, 40, 46]. Assuming a Gaussian form, we have

$$g_1^{\text{pdf}} = \frac{\langle k_\perp^2 \rangle_{Q_0}}{4}, \quad g_1^{\text{ff}} = \frac{\langle p_T^2 \rangle_{Q_0}}{4z^2}, \quad g_1^{\text{sivers}} = \frac{\langle k_{s\perp}^2 \rangle_{Q_0}}{4}, \quad (24)$$

where  $\langle k_\perp^2 \rangle_{Q_0}$ ,  $\langle p_T^2 \rangle_{Q_0}$ , and  $\langle k_{s\perp}^2 \rangle_{Q_0}$  are the relevant averaged intrinsic transverse momenta squared for TMDPDFs, TMDFFs, and the quark Sivers functions at the momentum scale  $Q_0$ , respectively.

Once we resort to such an intuitive interpretation and further choose  $Q_0 = \sqrt{2.4}$  GeV, the typical virtuality scale in the HERMES experiments,  $\langle k_\perp^2 \rangle_{Q_0}$  and  $\langle p_T^2 \rangle_{Q_0}$  have been extracted from the HERMES experimental data by various groups [55–58]. At present, values in the following ranges can give an equally good description of the data:

$$\langle k_\perp^2 \rangle_{Q_0} = 0.25 - 0.44 \text{ GeV}^2, \quad \langle p_T^2 \rangle_{Q_0} = 0.16 - 0.20 \text{ GeV}^2. \quad (25)$$

On the other hand, the universal parameter  $g_2$  has been extracted mainly from the DY lepton pair and  $W/Z$  production. The value of  $g_2$  is intimately connected to the value  $b_{\max}$  one is using. In Ref. [51], Konychev and Nadolsky have shown that the best fit of the experimental data can be reached if one chooses  $b_{\max} = 1.5$  GeV $^{-1}$ , and the fitted  $g_2$  is given by

$$g_2 = 0.184 \pm 0.018 \text{ GeV}^2. \quad (26)$$

In our work, we will try to tune the three parameters  $\langle k_\perp^2 \rangle_{Q_0}$ ,  $\langle p_T^2 \rangle_{Q_0}$ , and  $g_2$  within their current extracted ranges, Eqs. (25) and (26), to see if we can indeed reconcile the SIDIS process and the DY-type processes, and to test if we can describe all the SIDIS, DY lepton pair, and  $W/Z$  production data. Indeed, we find the following parameters can do a rather reasonable job:

$$\langle k_\perp^2 \rangle_{Q_0} = 0.38 \text{ GeV}^2, \quad \langle p_T^2 \rangle_{Q_0} = 0.19 \text{ GeV}^2, \quad g_2 = 0.16 \text{ GeV}^2. \quad (27)$$

The variation of the non-perturbative parameters that enter into the evolution of TMDs should not affect the shape of the kernel in the perturbative region  $1/b \gg \Lambda_{\text{QCD}}$ , where no non-perturbative model is needed. In other words, the

relative change of the parameters  $b_{\max}$  and  $g_2$  should conspire in such a way that the kernel in the perturbative region is not spoiled. We have checked this fact explicitly at NLL accuracy for our tuned parameters  $b_{\max} = 1.5 \text{ GeV}^{-1}$  and  $g_2 = 0.16$ , and found that this is indeed the case. In the next subsection we show that the implementation of the Sudakov factor with the above  $g_2$  parameter leads to a reasonably good description of all the experimental data on SIDIS, DY lepton pair and  $W/Z$  boson production, and hence a more solid extraction of the Sivers asymmetry.

## B. Transverse momentum distribution

Here we first review the QCD factorization formalism for the transverse momentum distribution of hadron production in SIDIS, DY lepton pair and  $W/Z$  boson production in  $pp$  collisions. We then demonstrate that the QCD factorization formalism with the evolution implemented as in Eq. (17) and the tuned non-perturbative Sudakov factor with parameters given in Eq. (27) leads to a reasonably good description of the experimental data on SIDIS, DY lepton pair, and  $W/Z$  production.

We start with single hadron production in SIDIS: the scattering processes of a lepton  $e$  on a hadron  $A$ ,

$$e(\ell) + A(P) \rightarrow e(\ell') + h(P_h) + X, \quad (28)$$

where we use  $A$  (also  $B$  below) generically to represent the incoming hadrons, and  $h$  is the observed hadron with momentum  $P_h$ . We define the virtual photon momentum  $q = \ell - \ell'$  and its invariant mass  $Q^2 = -q^2$ , and adopt the usual SIDIS variables [61]:

$$S_{ep} = (P + \ell)^2, \quad x_B = \frac{Q^2}{2P \cdot q}, \quad y = \frac{P \cdot q}{P \cdot \ell} = \frac{Q^2}{x_B S_{ep}}, \quad z_h = \frac{P \cdot P_h}{P \cdot q}. \quad (29)$$

The so-called hadron multiplicity distribution is defined as

$$\frac{dN}{dz_h d^2 P_{h\perp}} = \frac{d\sigma}{dx_B dQ^2 dz_h d^2 P_{h\perp}} \bigg/ \frac{d\sigma}{dx_B dQ^2}, \quad (30)$$

where the numerator and denominator are given by

$$\frac{d\sigma}{dx_B dQ^2 dz_h d^2 P_{h\perp}} = \frac{\sigma_0^{\text{DIS}}}{2\pi} \sum_q e_q^2 \int_0^\infty db b J_0(P_{h\perp} b / z_h) f_{q/A}(x_B, b; Q) D_{h/q}(z_h, b; Q), \quad (31)$$

$$\frac{d\sigma}{dx_B dQ^2} = \sigma_0^{\text{DIS}} \sum_q e_q^2 f_{q/A}(x_B, Q), \quad (32)$$

with  $\sigma_0^{\text{DIS}} = 2\pi\alpha_{\text{em}}^2 [1 + (1 - y)^2] / Q^4$ . Here,  $f_{q/A}(x_B, Q)$  is the collinear PDF at momentum scale  $Q$ , while  $f_{q/A}(x_B, b; Q)$  and  $D_{h/q}(z_h, b; Q)$  are the evolved TMDPDFs and TMDFFs given by Eqs. (21) and (22), respectively. It is worth pointing out that we have taken the hard factor at LO (equal to 1) in the above TMD factorization formalism as in Eq. (31) and throughout the paper, to be consistent with the fact that we use the LO coefficient function in Eqs. (12) - (14). Notice as well that the relevant soft function for each process, either DY or SIDIS, which accounts for the soft gluon radiation, is already included in the proper definition of the TMDs in each case [26, 49].

On the other hand, for Drell-Yan lepton pair production,  $A(P_A) + B(P_B) \rightarrow [\gamma^* \rightarrow] \ell^+ \ell^- (y, Q, p_\perp) + X$ , with  $y, Q, p_\perp$  being the rapidity, invariant mass and transverse momentum of the pair, respectively, the spin-averaged differential cross section can be written as [62]

$$\frac{d\sigma}{dQ^2 dy d^2 p_\perp} = \frac{\sigma_0^{\text{DY}}}{2\pi} \sum_q e_q^2 \int_0^\infty db b J_0(p_\perp b) f_{q/A}(x_a, b; Q) f_{\bar{q}/B}(x_b, b; Q). \quad (33)$$

Here  $\sigma_0^{\text{DY}} = 4\pi\alpha_{\text{em}}^2 / 3sQ^2 N_c$ ,  $s = (P_A + P_B)^2$  is the center-of-mass (CM) energy squared, and the parton momentum fractions  $x_a$  and  $x_b$  are given by

$$x_a = \frac{Q}{\sqrt{s}} e^y, \quad x_b = \frac{Q}{\sqrt{s}} e^{-y}. \quad (34)$$

Likewise,  $f_{q/A}(x_a, b; Q)$  and  $f_{\bar{q}/B}(x_b, b; Q)$  are the QCD evolved TMDPDFs in Eq. (21). Similarly, for  $W/Z$  production,  $A(P_A) + B(P_B) \rightarrow W/Z(y, p_\perp) + X$ , the differential cross sections are given by [16, 63]

$$\frac{d\sigma^W}{dyd^2p_\perp} = \frac{\sigma_0^W}{2\pi} \sum_{q,q'} |V_{qq'}|^2 \int_0^\infty db b J_0(q_\perp b) f_{q/A}(x_a, b; Q) f_{q'/B}(x_b, b; Q), \quad (35)$$

$$\frac{d\sigma^Z}{dyd^2p_\perp} = \frac{\sigma_0^Z}{2\pi} \sum_q (V_q^2 + A_q^2) \int_0^\infty db b J_0(q_\perp b) f_{q/A}(x_a, b; Q) f_{\bar{q}/B}(x_b, b; Q), \quad (36)$$

where  $V_{qq'}$  are the CKM matrix elements for the weak interaction, and  $V_q$  and  $A_q$  are the vector and axial couplings of the  $Z$  boson to the quark, respectively. The LO cross sections  $\sigma_0^W$  and  $\sigma_0^Z$  have the following form

$$\sigma_0^W = \frac{\sqrt{2}\pi G_F M_W^2}{sN_c}, \quad \sigma_0^Z = \frac{\sqrt{2}\pi G_F M_Z^2}{sN_c}, \quad (37)$$

where  $G_F$  is the Fermi weak coupling constant, and  $M_W$  ( $M_Z$ ) is the mass of the  $W$  ( $Z$ ) boson.

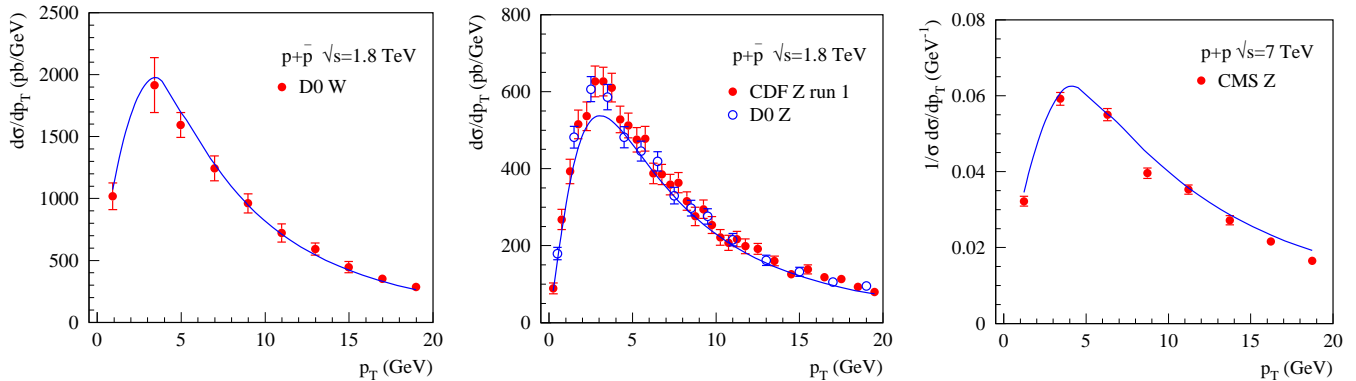


FIG. 1. Comparison of theoretical results to  $W$  [67] (left) and  $Z$  [68, 69] (middle) production in  $p + \bar{p}$  collisions at  $\sqrt{s} = 1.8$  TeV, and  $Z$  production [70] (right) in  $p + p$  collisions at  $\sqrt{s} = 7$  TeV.

To compare with experimental data, we use the unpolarized parton distribution functions  $f_{q/A}(x, Q)$  as given by the MSTW2008 parametrization [64] and the DSS unpolarized fragmentation functions  $D_{h/q}(z, Q)$  [65]. It is important to remember that our QCD factorization formalism based on TMDs is only applicable in the kinematic region where  $p_\perp \ll Q$  [26]. To describe the large  $p_\perp \sim Q$  region, one needs the complete next-to-leading order calculation, more precisely the so-called  $Y$ -term [39–41, 66]. To be consistent with our formalism, we thus restrict our comparison with the experimental data as follows: for  $W/Z$  boson production, we choose  $p_\perp \leq 20$  GeV; for  $DY$  dilepton production, we have  $p_\perp \leq 1.3$  GeV; for hadron production at COMPASS with  $\langle Q^2 \rangle = 7.57$  GeV<sup>2</sup>, we choose  $P_{h\perp} \leq 0.7$  GeV; for hadron production at HERMES with  $\langle Q^2 \rangle = 2.45$  GeV<sup>2</sup>, we choose  $P_{h\perp} \leq 0.6$  GeV such that we still have enough experimental data for the analysis.

We first compare in Fig. 1 our calculation, based on the QCD factorization formalism, Eqs. (35) and (36), with  $W/Z$  production at both the Tevatron and LHC energies. With QCD evolved TMDPDFs given in Eq. (21) and the tuned parameters for the Sudakov factor in Eq. (27), we plot the  $W$  and  $Z$  boson differential cross section as a function of transverse momentum  $p_\perp$ . The left and middle panels of Fig. 1 are the comparisons with the  $W/Z$  measurements [67–69] in  $p + \bar{p}$  collisions at the Tevatron energy  $\sqrt{s} = 1.8$  TeV. In the right panel of Fig. 1 we compare with the most recent  $Z$  boson measurement [70] in  $p + p$  collisions from the CMS collaboration at LHC energy  $\sqrt{s} = 7$  TeV. Our formalism gives a reasonably good description of the  $W/Z$  boson production at both the Tevatron and LHC energies.

Next, we compare our calculation for the  $DY$  lepton pair production with the fixed-target Fermilab experimental data at different CM energies  $\sqrt{s} = 19.4, 23.8, 27.4$  for the E288 collaboration [71] and at  $\sqrt{s} = 38.8$  GeV for the E605 collaboration [72], see Fig. 2. Since these experiments were really performed for  $p + Cu$  collisions, we use the EKS98 parametrization [73] for the collinear nuclear PDFs in the nucleus  $Cu$ . For both  $\sqrt{s} = 19.4$  and  $23.8$  GeV, the curves from top to bottom correspond to the different invariant mass bins, i.e.,  $Q \in [4, 5], [5, 6], [6, 7], [7, 8],$  and  $[8, 9]$  GeV. For  $\sqrt{s} = 27.4$  GeV, we have  $Q \in [5, 6], [6, 7], [7, 8],$  and  $[8, 9]$  GeV. Finally, for  $\sqrt{s} = 38.8$  GeV the mass ranges are:  $Q \in [7, 8], [8, 9], [10.5, 11.5], [11.5, 13.5],$  and  $[13.5, 18]$  GeV. As can be seen, our QCD formalism gives a reasonably good description of the Drell-Yan dilepton production in all the measured mass ranges.

Let us now turn to the hadron multiplicity distribution in the SIDIS processes. In Fig. 3, we compare our calculations with the recent COMPASS experimental data for the charged hadron multiplicity distribution [74] at  $\langle Q^2 \rangle = 7.57$

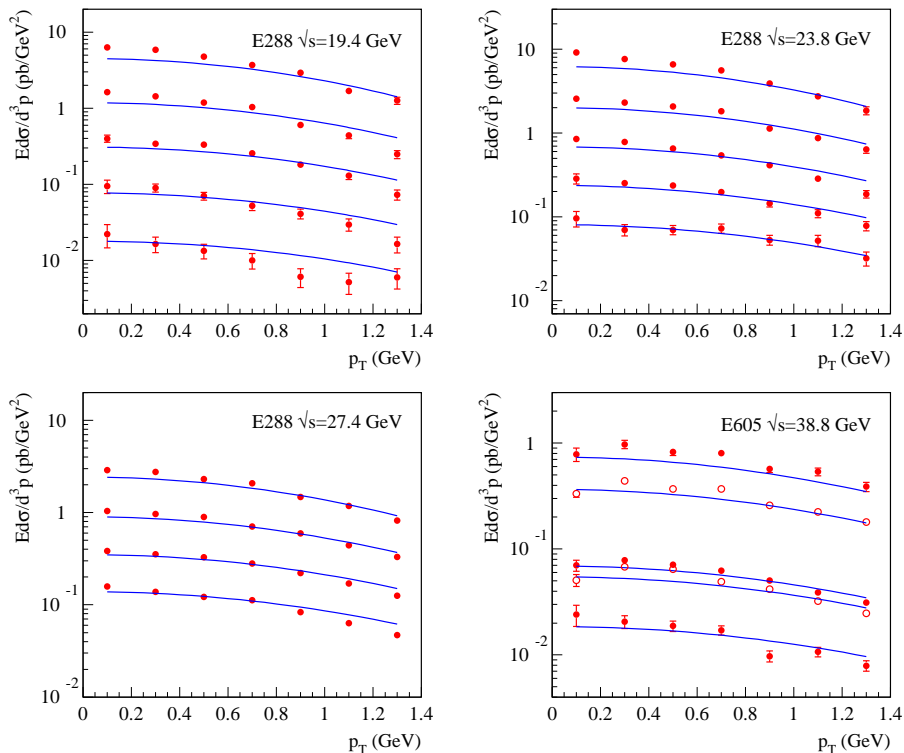


FIG. 2. The first three plots show comparisons with the Fermilab E288 Drell-Yan dilepton data at different CM energies  $\sqrt{s} = 19.4$  (left), 23.8, and 27.4 GeV [71]. The data points from top to bottom correspond to different invariant mass  $Q$  of the lepton pair. For the top two plots, they are: [4, 5], [5, 6], [6, 7], [7, 8], and [8, 9] GeV. For the left bottom plot, it starts with the [5, 6] GeV range (no [4, 5] GeV range). The right bottom plot is the comparison with the Fermilab E605 Drell-Yan dilepton data at CM energy  $\sqrt{s} = 38.8$  GeV [72]. Again the mass ranges are: [7, 8], [8, 9], [10.5, 11.5], [11.5, 13.5], and [13.5, 18] GeV.

$\text{GeV}^2$  and  $\langle x_B \rangle = 0.093$  for a deuteron target. The data points from top to bottom correspond to different  $z_h$  regions:  $z_h \in [0.2, 0.25]$ ,  $[0.25, 0.3]$ ,  $[0.3, 0.35]$ ,  $[0.35, 0.4]$ ,  $[0.4, 0.5]$ ,  $[0.5, 0.6]$ ,  $[0.6, 0.7]$ , and  $[0.7, 0.8]$ . We find that for both negative and positive charged hadrons the QCD formalism in Eq. (30) gives a good description for the  $P_{h\perp}$ -dependence of the hadron multiplicity distribution.

Finally, in Fig. 4 we compare our calculation with the HERMES multiplicity distribution data [75] for a proton target at  $\langle Q^2 \rangle = 2.45 \text{ GeV}^2$  and  $\langle x_B \rangle = 0.117$ . The data points from top to bottom correspond to different  $z_h$  regions:  $z_h \in [0.2, 0.3]$ ,  $[0.3, 0.4]$ ,  $[0.4, 0.6]$ , and  $[0.6, 0.8]$ . We find that our formalism still gives a reasonable description for  $\pi^-$  multiplicity distribution data as a function of  $P_{h\perp}$ , though  $\pi^+$  becomes worse when going to the high  $z_h$  region. Note, however, that the normalization of such distributions is related to the fragmentation functions [75].

In summary we find that our proposed non-perturbative Sudakov factor in Eq. (27) along with  $b_{\text{max}} = 1.5 \text{ GeV}^{-1}$  gives a reasonably good description of the hadron multiplicity distribution in SIDIS at rather low  $Q$ , DY lepton pair production at intermediate  $Q$ , and  $W/Z$  production at high  $Q$  from rather low CM energies up to the LHC energies. Even though the description is not perfect, one has to keep in mind that our QCD formalism is the very first attempt to use a universal form to describe the experimental data on both SIDIS and DY-type processes. At the moment, we are implementing the evolution at NLL accuracy along with the LO coefficient functions. All of these could be further improved, and a first attempt to implement the approach presented in [29] is being pursued in [76]. Another important consequence is that since the parameter  $g_2$  is a universal parameter, i.e. independent of the spin, we can then use the same  $g_2$  to extract the Siversons functions from the current Siversons asymmetry measurements in SIDIS. This will be the main focus of the next section.

### III. QCD EVOLUTION OF TMDS: THE SIVERS EFFECT

In this section we will first extract the quark Siversons functions from the Siversons asymmetry measurements in SIDIS from JLab, HERMES, and COMPASS experiments. We will then make predictions for the Siversons asymmetries of DY dilepton and  $W$  boson production, to be compared with the future measurements.

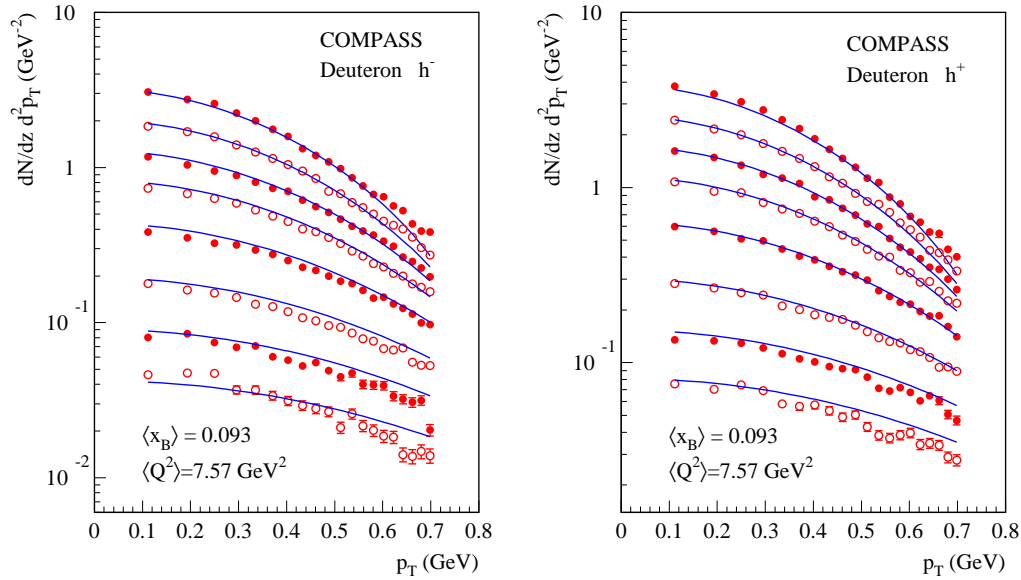


FIG. 3. Comparison of the theoretical results with the COMPASS data (deuteron target) [74] at  $\langle Q^2 \rangle = 7.57 \text{ GeV}^2$  and  $\langle x_B \rangle = 0.093$ . The data points from top to bottom correspond to different  $z_h$  regions: [0.2, 0.25], [0.25, 0.3], [0.3, 0.35], [0.35, 0.4], [0.4, 0.5], [0.5, 0.6], [0.6, 0.7], and [0.7, 0.8].

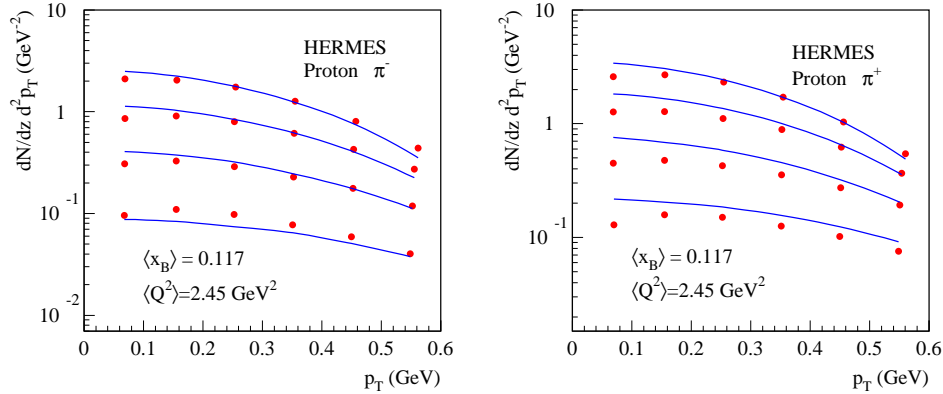


FIG. 4. Comparison of theoretical results with the HERMES data (proton target) [75] at  $\langle Q^2 \rangle = 2.45 \text{ GeV}^2$  and  $\langle x_B \rangle = 0.117$ . The data points from top to bottom correspond to different  $z_h$  regions: [0.2, 0.3], [0.3, 0.4], [0.4, 0.6], and [0.6, 0.8].

### A. Global fitting of Siverson asymmetries in SIDIS

Here we apply our QCD evolution formalism for the Siverson effect in SIDIS and use it to extract the quark Siverson functions from the experimental data. The differential SIDIS cross section on a transversely polarized nucleon target can be written as [13, 77, 78]

$$\frac{d\sigma}{dx_B dy dz_h d^2 P_{h\perp}} = \sigma_0(x_B, y, Q^2) \left[ F_{UU} + \sin(\phi_h - \phi_s) F_{UT}^{\sin(\phi_h - \phi_s)} \right], \quad (38)$$

where  $\sigma_0 = \frac{2\pi\alpha_{em}^2}{Q^2 y} (1 + (1-y)^2)$ , and  $\phi_s$  and  $\phi_h$  are the azimuthal angles for the nucleon spin and the transverse momentum of the outgoing hadron, respectively.  $F_{UU}$  and  $F_{UT}^{\sin(\phi_h - \phi_s)}$  are the spin-averaged and transverse spin-



dependent structure functions that have the expressions:

$$F_{UU} = \frac{1}{2\pi} \int_0^\infty db b J_0(P_{h\perp} b/z_h) \sum_q e_q^2 f_{q/A}(x_B, b; Q) D_{h/q}(z_h, b; Q), \quad (39)$$

$$F_{UT}^{\sin(\phi_h - \phi_s)} = - \int \frac{d^2b}{(2\pi)^2} e^{iP_{h\perp} \cdot b/z_h} \hat{P}_{h\perp}^\alpha \sum_q e_q^2 f_{1T, \text{SIDIS}}^{\perp q(\alpha)}(x_B, b; Q) D_{h/q}(z_h, b; Q), \quad (40)$$

where  $\hat{P}_{h\perp}$  is the unit vector along the hadron transverse momentum  $P_{h\perp}$ . If we include the QCD evolution of both the quark Sivers function and the fragmentation function as in Eqs. (22) and (23) into Eq. (40), we can eventually write  $F_{UT}^{\sin(\phi_h - \phi_s)}$  as

$$F_{UT}^{\sin(\phi_h - \phi_s)} = \frac{1}{4\pi z_h^2} \int_0^\infty db b^2 J_1(P_{h\perp} b/z_h) \sum_q e_q^2 T_{q,F}(x_B, x_B, c/b_*) D_{h/q}(z_h, c/b_*) \\ \times \exp \left\{ - \int_{c^2/b_*^2}^{Q^2} \frac{d\mu^2}{\mu^2} \left( A \ln \frac{Q^2}{\mu^2} + B \right) \right\} \exp \left\{ -b^2 \left( g_1^{\text{ff}} + g_1^{\text{sivers}} + g_2 \ln \frac{Q}{Q_0} \right) \right\}, \quad (41)$$

with  $J_1$  being the Bessel function of the first order. The Sivers asymmetry  $A_{UT}^{\sin(\phi_h - \phi_s)}$  is defined as

$$A_{UT}^{\sin(\phi_h - \phi_s)} = \frac{\sigma_0(x_B, y, Q^2) F_{UT}^{\sin(\phi_h - \phi_s)}}{\sigma_0(x_B, y, Q^2) F_{UU}}. \quad (42)$$

If we want to use the above QCD formalism (with QCD evolution of TMDs included) to describe the Sivers asymmetries in SIDIS, we have to parametrize the usual Qiu-Sterman functions  $T_{q,F}(x, x, \mu)$ . For this part, following [79], we assume they are proportional to the usual unpolarized collinear PDFs as

$$T_{q,F}(x, x, \mu) = N_q \frac{(\alpha_q + \beta_q)^{(\alpha_q + \beta_q)}}{\alpha_q^{\alpha_q} \beta_q^{\beta_q}} x^{\alpha_q} (1-x)^{\beta_q} f_{q/A}(x, \mu). \quad (43)$$

We will have  $\alpha_u, \alpha_d, N_u, N_d$  for  $u$  and  $d$  quarks, and  $N_{\bar{u}}, N_{\bar{d}}, N_s, N_{\bar{s}}, \alpha_{\text{sea}}$  for sea quarks. At the same time, we choose the same  $\beta_q \equiv \beta$  for all quark flavors. Including  $\langle k_{s\perp}^2 \rangle = 4g_1^{\text{sivers}}$  in the non-perturbative Sudakov factor Eq. (23), we have in total 11 fitting parameters.

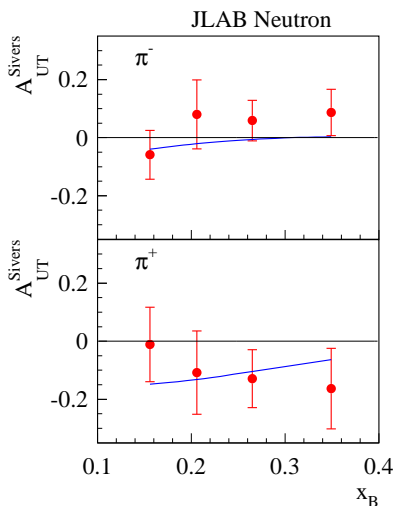


FIG. 5. Results obtained from the TMD evolution fit of the SIDIS  $A_{UT}^{\sin(\phi_h - \phi_s)}$  Sivers asymmetries are compared with the JLab experimental data [20] for charged pion production on a neutron target.

We use the MINUIT package to perform a global fit of the Sivers asymmetries data in SIDIS. To be consistent with the region of applicability of our QCD factorization formalism while still having enough experimental data in our analysis, we restrict our fit to the same transverse momentum region as specified in last section for the unpolarized

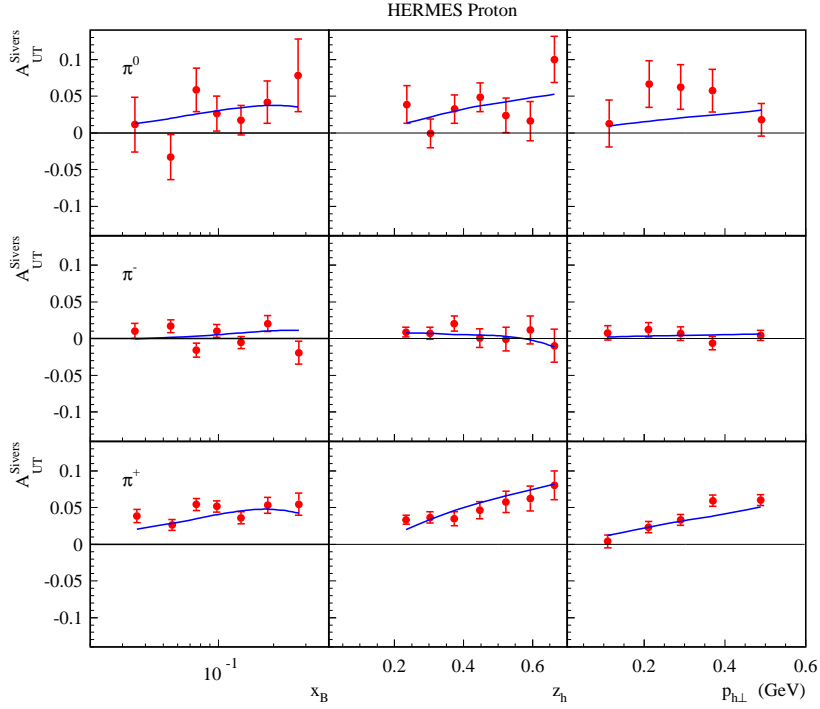


FIG. 6. Results obtained from the TMD evolution fit of the SIDIS  $A_{UT}^{\text{Sivers}(\phi_h - \phi_s)}$  Sivers asymmetries are compared with the HERMES experimental data [17] for neutral and charged pion production.

differential cross section: for hadron production at JLab [20] with  $\langle Q^2 \rangle = 1.38 - 2.68 \text{ GeV}^2$  we choose  $P_{h\perp} \leq 0.5 \text{ GeV}$ ; for hadron production at HERMES [17] with  $\langle Q^2 \rangle \approx 2.45 \text{ GeV}^2$ , we choose  $P_{h\perp} \leq 0.6 \text{ GeV}$ ; and for the COMPASS experimental data [18, 19] with  $\langle Q^2 \rangle \approx 3 - 5 \text{ GeV}^2$ , we choose  $P_{h\perp} \leq 0.7 \text{ GeV}$ . For the transversely polarized neutron and deuteron targets, we use isospin symmetry to relate the quark Sivers functions to those in the proton target. By simultaneously fitting pion, kaon, and charged hadron experimental data [17–20] from JLab, HERMES, and COMPASS, we obtain an acceptable overall description of the experimental data with the total  $\chi^2 \approx 300$  for 241 data points, and thus  $\chi^2/d.o.f. = 1.3$ . The fitted parameters are given in the Table. I.

TABLE I. Best values of the free parameters for the Sivers function from our fit to SIDIS data [17–20] on  $A_{UT}^{\text{Sivers}(\phi_h - \phi_s)}$ .

| $\chi^2/d.o.f. = 1.3$          |   |               |                            |
|--------------------------------|---|---------------|----------------------------|
| $\alpha_u$                     | $1.051^{+0.192}_{-0.180}$               | $\alpha_d$    | $1.552^{+0.303}_{-0.275}$  |
| $\alpha_{sea}$                 | $0.851^{+0.307}_{-0.305}$               | $\beta$       | $4.857^{+1.534}_{-1.395}$  |
| $N_u$                          | $0.106^{+0.011}_{-0.009}$               | $N_d$         | $-0.163^{+0.039}_{-0.046}$ |
| $N_{\bar{u}}$                  | $-0.012^{+0.018}_{-0.020}$              | $N_{\bar{d}}$ | $-0.105^{+0.043}_{-0.060}$ |
| $N_s$                          | $0.103^{+0.548}_{-0.604}$               | $N_{\bar{s}}$ | $-1.000 \pm 1.757$         |
| $\langle k_{s\perp}^2 \rangle$ | $0.282^{+0.073}_{-0.066} \text{ GeV}^2$ |               |                            |

Comparison of the fits to the experimental data are presented in Figs. 5 - 10, with the solid curves representing our fitted theoretical results. In Fig. 5 we show the comparison with the JLab experimental data [20] for charged pion production on a neutron target. JLab experimental data have a relatively large error bar for the asymmetries and have only the  $x_B$ -dependence of the Sivers asymmetries. On the other hand, both HERMES and COMPASS experimental data have the Sivers asymmetries as functions of  $x_B$ ,  $z_h$ , and  $P_{h\perp}$ , respectively. In Figs. 6 and 7 we show the results obtained from our fit compared with the HERMES experimental data [17] for pion and kaon production on a proton target, respectively. In Figs. 8 and 9 we present the comparison with the COMPASS experimental data for charged pion and kaon production on a deuteron target [18]. Finally, in Fig. 10 we show the comparison with the COMPASS experimental data for charged hadron production on a proton target [19]. One sees that the fit is of rather good quality. Even though the  $\chi^2/d.o.f.$  is slightly larger than earlier Gaussian-form fits for the TMDs [78], we feel more confident about our results as they are based on a QCD formalism which can give a rather good description for

all the corresponding unpolarized differential cross sections.

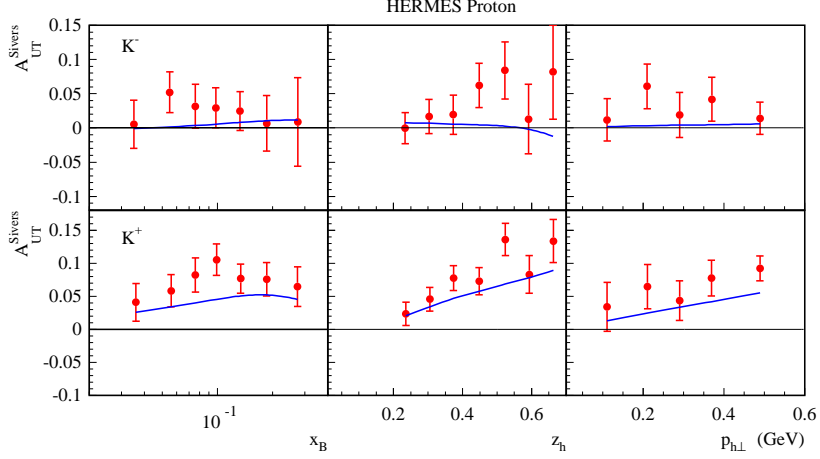


FIG. 7. Results obtained from the TMD evolution fit of the SIDIS  $A_{UT}^{\text{Sivers}(\sin(\phi_h - \phi_s))}$  Sivers asymmetries are compared with the HERMES experimental data [17] for kaon production.

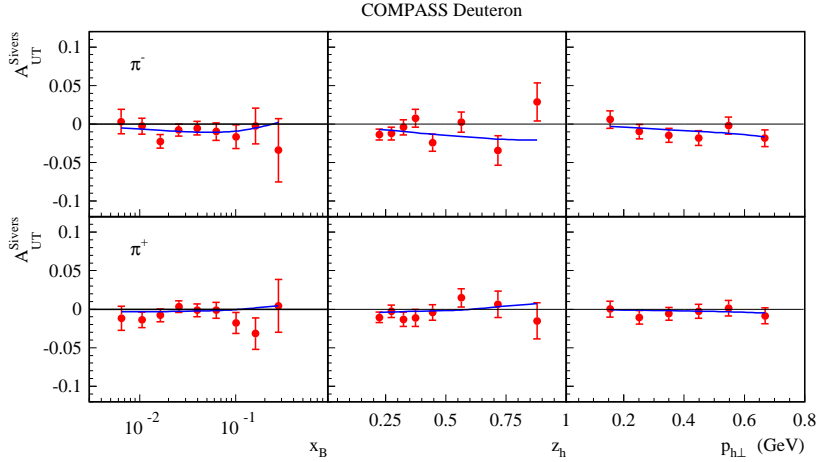


FIG. 8. Results obtained from the TMD evolution fit of the SIDIS  $A_{UT}^{\text{Sivers}(\sin(\phi_h - \phi_s))}$  Sivers asymmetries are compared with the COMPASS experimental data [18] for charged pion production on a Deuteron target.

In Fig. 11, we show the Qiu-Sterman function  $T_{q,F}(x, x, Q)$  extracted from our fits for  $u$ ,  $d$ , and  $s$  quark flavors as a function of parton momentum fraction  $x$  at a scale  $Q^2 = 2.4 \text{ GeV}^2$ . We find  $T_{u,F}(x, x, Q)$  and  $T_{d,F}(x, x, Q)$  have a similar size but opposite sign, which is consistent with previous extractions from the SIDIS process [48, 78, 80]. The current extraction with the limited kinematic coverage from the experimental data can only constrain reasonably well the  $u$  and  $d$  quark Sivers functions. All of the sea quark Sivers functions are not constrained well. For example, even if we neglect all the sea quark Sivers functions in our formalism, we obtain a similar  $\chi^2/d.o.f.$ . In this respect, the future planned electron-ion collider experiments and the DY and  $W$  boson production [4, 21–24] should provide us with better constraints on the sea quark Sivers functions.

## B. Predictions for the Sivers effect in DY production

One of the most important properties of the Sivers function is its time-reversal modified universality, which has been extensively studied in recent years. In particular, the Sivers function changes sign while keeping its magnitude when going from the SIDIS process to the DY processes. Testing this sign change has become one of the hot topics in hadron physics in recent years. There have been calculations for the Sivers asymmetries in DY production based on the naive parton model without QCD evolution of the TMDs, see [63, 81–83]. One of the most recent papers [48] has

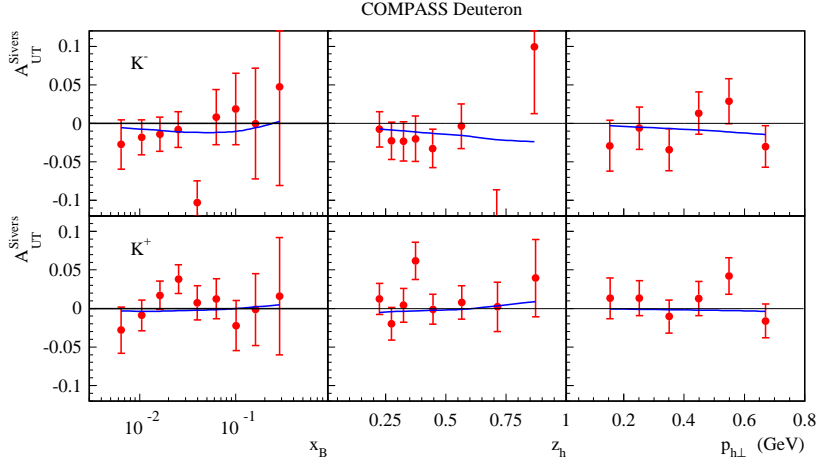


FIG. 9. Results obtained from the TMD evolution fit of the SIDIS  $A_{UT}^{\sin(\phi_h - \phi_s)}$  Sivers asymmetries are compared with the COMPASS experimental data [18] for kaon production on a Deuteron target.

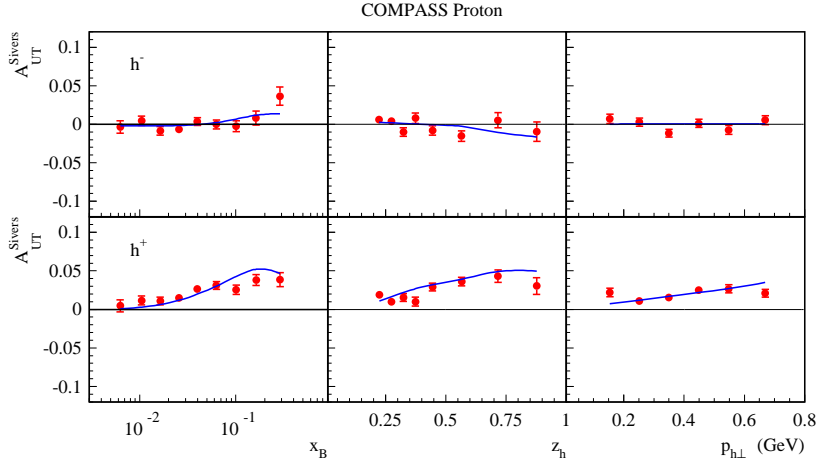


FIG. 10. Results obtained from the TMD evolution fit of the SIDIS  $A_{UT}^{\sin(\phi_h - \phi_s)}$  Sivers asymmetries are compared with the COMPASS experimental data [74] for charged hadron production on a proton target.

taken into account the QCD evolution of TMDs, in which the authors use a different Sudakov factor for the evolution in the region from the low  $Q$  to the intermediate  $Q \sim 10$  GeV, and in the region from the intermediate  $Q \sim 10$  GeV to high  $Q \sim M_{W/Z}$ . In this section, we will use the information on the Sivers functions obtained through our fit to make predictions for the Sivers asymmetries for both DY lepton pair and  $W$  boson production in  $pp$  collisions. Importantly, we are able to use the same universal Sudakov factor in the QCD evolution for the whole  $Q$  region: from low  $Q$  up to high  $Q \sim M_{W/Z}$ .

For Drell-Yan production in single transversely polarized  $p^\uparrow p$  collisions,  $A^\uparrow(P_A, s_\perp) + B(P_B) \rightarrow [\gamma^* \rightarrow] \ell^+ \ell^- (y, Q, q_\perp) + X$ , the unpolarized differential cross section at small  $p_\perp \ll Q$  is given by Eq. (33), while the spin-dependent cross section  $\Delta\sigma \equiv [\sigma(s_\perp) - \sigma(-s_\perp)]/2$  can be written as [25, 84]

$$\begin{aligned}
\frac{d\Delta\sigma}{dQ^2 dy d^2 p_\perp} &= \epsilon^{\alpha\beta} s_\perp^\alpha \sigma_0^{\text{DY}} \int \frac{d^2 b}{(2\pi)^2} e^{i p_\perp \cdot b} \sum_q e_q^2 f_{1T, \text{DY}}^{\perp, q(\beta)}(x_a, b; Q) f_{\bar{q}/B}(x_b, b; Q), \\
&= -\frac{\sigma_0^{\text{DY}}}{4\pi} \int_0^\infty db b^2 J_1(p_\perp b) \sum_q e_q^2 T_{q, F}(x_a, x_a, c/b^*) f_{\bar{q}/B}(x_b, c/b^*) \\
&\quad \times \exp \left\{ -\int_{c/b^*}^Q \frac{d\mu^2}{\mu^2} \left( A \ln \frac{Q^2}{\mu^2} + B \right) \right\} \exp \left\{ -b^2 \left( g_1^{\text{pdf}} + g_1^{\text{sivers}} + g_2 \ln \frac{Q}{Q_0} \right) \right\}. \quad (44)
\end{aligned}$$

To arrive at the second expression in Eq. (44), we first apply the sign change for the Sivers functions between the

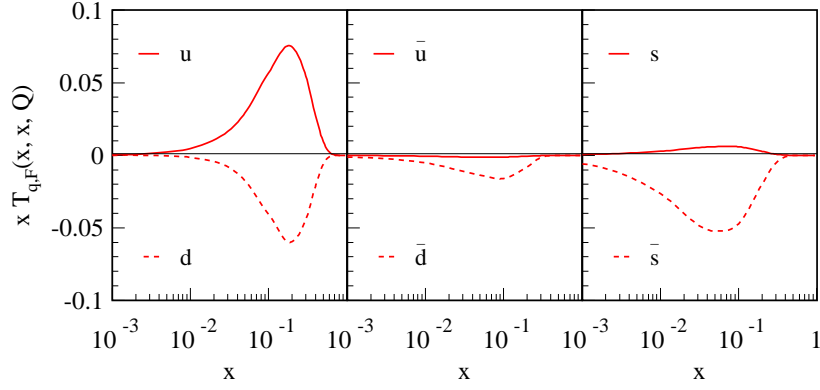


FIG. 11. Qiu-Sterman function  $T_{q,F}(x, x, Q)$  for  $u$ ,  $d$ , and  $s$  flavors at a scale  $Q^2 = 2.4 \text{ GeV}^2$ , as extracted by our simultaneous fit of JLab, HERMES, and COMPASS data.

SIDIS and the DY processes

$$f_{1T,DY}^{\perp,q(\beta)}(x_a, b; Q) = -f_{1T,SIDIS}^{\perp,q(\beta)}(x_a, b; Q). \quad (45)$$

We then use Eq. (23) and Eq. (44) and follow the experimental convention to choose the pair's transverse momentum  $p_{\perp}$  along the  $x$ -direction, while the spin vector  $s_{\perp}$  is along  $y$ -direction [10, 85] and the transversely polarized proton is moving in the  $+z$ -direction. The single transverse spin asymmetry for DY production is given by

$$A_N = \frac{d\Delta\sigma}{dQ^2 dy d^2p_{\perp}} \bigg/ \frac{d\sigma}{dQ^2 dy d^2p_{\perp}}. \quad (46)$$

It is important to realize that the  $A_N$  defined above is opposite to the so-called weighted asymmetry  $A_N^{\sin(\phi_{\gamma}-\phi_s)}$  defined in the literature, see, e.g., Refs. [63, 83].

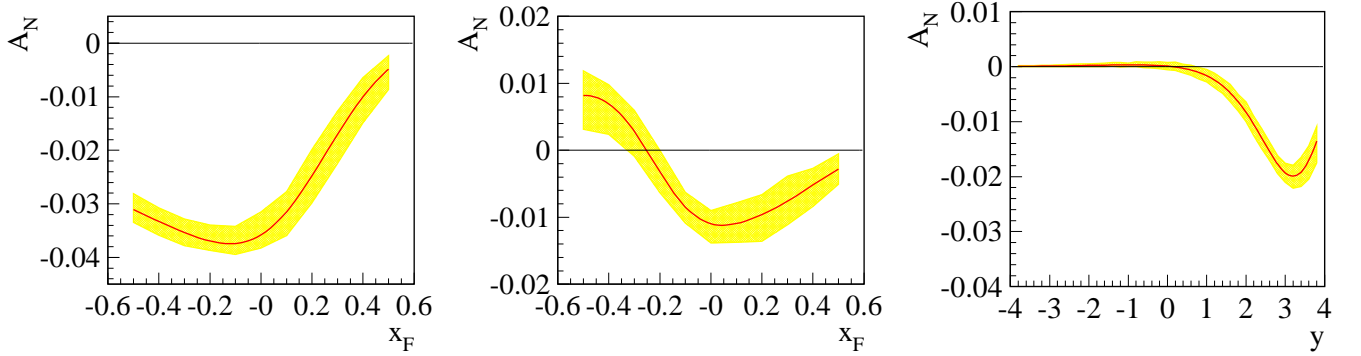


FIG. 12. Estimated Siverson asymmetries for DY lepton pair production. Left plot:  $A_N$  in  $p^{\uparrow}\pi^-$  collisions as a function of  $x_F$  at COMPASS energy  $\sqrt{s} = 18.9 \text{ GeV}$ . Middle plot:  $A_N$  in  $p^{\uparrow}p$  collisions is plotted as a function of  $x_F$  at Fermilab energy  $\sqrt{s} = 15.1 \text{ GeV}$ . Right plot:  $A_N$  in  $p^{\uparrow}p$  collisions is plotted as a function of the pair's rapidity  $y$  at RHIC energy  $\sqrt{s} = 510 \text{ GeV}$ . We have integrated over the pair's transverse momentum  $0 < p_{\perp} < 1 \text{ GeV}$  in the invariant mass range  $4 < Q < 9 \text{ GeV}$ .

There are several planned experiments to measure the  $A_N$  for DY lepton pair production. The COMPASS collaboration at CERN will use a 190 GeV  $\pi^-$  beam to scatter on the polarized proton target [21], which corresponds to a CM energy  $\sqrt{s} = 18.9 \text{ GeV}$ . At Fermilab, one can use the 120 GeV proton beam in the main injector. There are two proposals corresponding to either a polarized proton beam [22] or a polarized proton target [23]. In both cases, the CM energy is  $\sqrt{s} = 15.1 \text{ GeV}$ . Finally, a DY measurement is also planned at RHIC [4, 24]. In the following, we will present an estimate of the Siverson asymmetry based on our evolution approach. For better comparison, we will always present the asymmetry in the center-of-mass frame of the colliding particles. We further choose the transversely polarized proton to move in the  $+z$  direction, while the other unpolarized particle ( $\pi^-$  for COMPASS and the unpolarized proton for Fermilab and RHIC) moves in the  $-z$  direction. We define

$$x_F = x_a - x_b, \quad (47)$$

which is the Feynman- $x$  at tree level with  $x_{a,b}$  given by Eq. (34). Here,  $x_a$  is always the parton momentum fraction in the transversely polarized proton, while  $x_b$  is the parton momentum fraction in the other unpolarized particle. It is important to mention that these conventions could differ from those used in some experiments [21, 23].

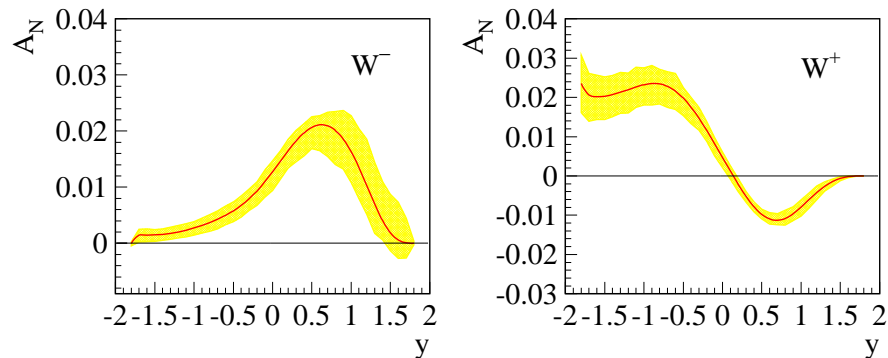


FIG. 13. Estimated Siverson asymmetries as a function of rapidity  $y$  for  $W^-$  and  $W^+$  production at the RHIC energy  $\sqrt{s} = 510$  GeV. We have integrated over the transverse momentum for  $W$  boson in  $0 < p_\perp < 3$  GeV.

In Fig. 12 (left) we plot our predicted Siverson asymmetry  $A_N$  for DY lepton pair production as a function of  $x_F$  for COMPASS kinematics  $\sqrt{s} = 18.9$  GeV. For the pion beam, we use the PDFs in the pion extracted in [86]. We have integrated over the transverse momentum  $0 < p_\perp < 1$  GeV and invariant mass of the pair  $4 < Q < 9$  GeV. The solid curve corresponds to the calculation based on the best fit for the parameters in Table. I, while the shaded area in the figure corresponds to the  $1\sigma$  error in the fitted parameters. COMPASS projected their measurement around  $x_\pi - x_{p^\dagger} \approx 0.2$  (corresponding to our  $x_F = -0.2$  in Eq. (47)) [21]. The estimated asymmetry is around 3 – 4% and should be measurable.

In Fig. 12 (middle) we plot the estimated Siverson asymmetry for the Fermilab energy  $\sqrt{s} = 15.1$  GeV. The proposed “polarized beam” experiment [22] will correspond to the region  $0 < x_F < 0.6$ , while the proposed “polarized target” experiment [23] will roughly correspond to the region  $-0.6 < x_F < 0.1$  in our notation Eq. (47). The asymmetry is around 1 – 2%, which we hope it could be measured in the future. Finally, in Fig. 12 (right) we plot  $A_N$  as a function of the pair’s rapidity  $y$  at RHIC energy  $\sqrt{s} = 510$  GeV. We find that the asymmetry is around 2 – 3% in the forward rapidity, which should be measurable at RHIC.

Both the  $u$  and  $d$  quark Siverson functions contribute to the Siverson asymmetries in DY lepton pair production in  $pp$  collisions. Since  $u$  and  $d$  quark Siverson functions have opposite sign, as shown in last subsection, they partially cancel each other in their contribution to the DY asymmetry. In order to be able to test the sign change of the quark Siverson function separately,  $W$  boson asymmetries have been proposed [16] and have been planned at RHIC experiment [4]. In Fig. 13, we plot our predicted Siverson asymmetries  $A_N$  as a function of rapidity  $y$  for  $W^-$  and  $W^+$  boson production, respectively. The transverse momentum is integrated over  $0 < p_\perp < 3$  GeV and  $\sqrt{s} = 510$  GeV. The  $W^-$  asymmetry at forward rapidity is sensitive to the  $d$ -quark Siverson function. On the other hand, the  $W^+$  asymmetry is sensitive to  $u$  quark Siverson function at forward rapidity, while it receives contributions from both the  $\bar{d}$  and  $\bar{s}$  quark Siverson functions in the backward rapidity region. As we emphasized in the last subsection, sea quark Siverson functions are not constrained well by the current SIDIS data. Thus the future DY and  $W$  boson asymmetry measurements should provide valuable information on the sea quark Siverson functions. The  $W$  boson asymmetry can be quite large if calculated in a naive parton model without QCD evolution [16]. Once the QCD evolution is taken into account, the asymmetry is only about 2 – 3%. We hope it can still be measured by the RHIC experiments.

#### IV. SUMMARY

In this paper we studied the QCD evolution of Siverson asymmetries in both semi-inclusive deep inelastic scattering (SIDIS) and Drell-Yan production (DY). Since QCD evolution of TMDs involves both perturbative and non-perturbative parts, we verified that the non-perturbative part of the evolution kernel plays a very important role for phenomenological studies. Consequently, we placed special emphasis on the non-perturbative Sudakov factor in the evolution formalism. Since one essential part of this Sudakov factor is spin-independent, we first found a form which can describe reasonably well the experimental data for the transverse momentum distribution in SIDIS at relatively low momentum scale  $Q$ , DY lepton pair production at intermediate  $Q$ , and  $W/Z$  production at high  $Q$ . Once this part of the QCD evolution was fixed, we then used the same Sudakov factor to perform a global analysis of all the experimental data on the Siverson asymmetry from HERMES, COMPASS, and Jefferson Lab. We extracted the quark

Sivers functions in SIDIS from such a global fitting procedure and used them with a reversed sign to make predictions for the Sivers asymmetries for DY lepton pair and  $W$  production. We found that the valence quark region is well-constrained by existing measurements but the sea quark asymmetry cannot be reliably determined. Hence, it is important that these predictions be compared with the experimental measurements in the near future to not only test the sign change of the Sivers effect but also to determine much more accurately the Sivers functions for sea quarks.

## ACKNOWLEDGMENTS

M.G.E. and A.I. thank I. Scimemi for exchanging some thoughts regarding the content of this work compared with that of Ref. [76]. Z.K. thanks E. C. Aschenauer, A. Bacchetta, D. Boer, M. Boglione, L. Gamberg, A. Metz, A. Prokudin, J. Qiu, A. Signori, and W. Vogelsang for helpful discussions and useful comments. This research is supported by the US Department of Energy, Office of Science and in part by the LDRD program at LANL. It is also part of the research program of the “Stichting voor Fundamenteel Onderzoek der Materie (FOM)”, which is financially supported by the “Nederlandse Organisatie voor Wetenschappelijk Onderzoek (NWO)”, the US Department of Energy under Grant No. DE-SC0008745 and the Spanish MECO, Grant No. FPA2011-27853-CO2-02.

- 
- [1] D. Boer, M. Diehl, R. Milner, R. Venugopalan, W. Vogelsang, D. Kaplan, H. Montgomery and S. Vigdor *et al.*, arXiv:1108.1713 [nucl-th].
- [2] A. Accardi, J. L. Albacete, M. Anselmino, N. Armesto, E. C. Aschenauer, A. Bacchetta, D. Boer and W. Brooks *et al.*, arXiv:1212.1701 [nucl-ex].
- [3] M. Anselmino, H. Avakian, D. Boer, F. Bradamante, M. Burkardt, J. P. Chen, E. Cisbani and M. Contalbrigo *et al.*, Eur. Phys. J. A **47**, 35 (2011) [arXiv:1101.4199 [hep-ex]].
- [4] E. C. Aschenauer, A. Bazilevsky, K. Boyle, K. O. Eyster, R. Fatemi, C. Gagliardi, M. Grosse-Perdekamp and J. Lajoie *et al.*, arXiv:1304.0079 [nucl-ex].
- [5] J. -C. Peng and J. -W. Qiu, arXiv:1401.0934 [hep-ph].
- [6] S. J. Brodsky, D. S. Hwang and I. Schmidt, Phys. Lett. B **530**, 99 (2002) [hep-ph/0201296]; S. J. Brodsky, D. S. Hwang and I. Schmidt, Nucl. Phys. B **642**, 344 (2002) [hep-ph/0206259].
- [7] J. C. Collins, Phys. Lett. B **536**, 43 (2002) [hep-ph/0204004].
- [8] D. Boer, P. J. Mulders and F. Pijlman, Nucl. Phys. B **667**, 201 (2003) [hep-ph/0303034].
- [9] A. Metz, Phys. Lett. B **549**, 139 (2002) [hep-ph/0209054]; J. C. Collins and A. Metz, Phys. Rev. Lett. **93**, 252001 (2004) [hep-ph/0408249]; S. Meissner and A. Metz, Phys. Rev. Lett. **102**, 172003 (2009) [arXiv:0812.3783 [hep-ph]]; L. P. Gamberg, A. Mukherjee and P. J. Mulders, Phys. Rev. D **77**, 114026 (2008) [arXiv:0803.2632 [hep-ph]]; D. Boer, Z. -B. Kang, W. Vogelsang and F. Yuan, Phys. Rev. Lett. **105**, 202001 (2010) [arXiv:1008.3543 [hep-ph]].
- [10] Z. -B. Kang, J. -W. Qiu, W. Vogelsang and F. Yuan, Phys. Rev. D **83**, 094001 (2011) [arXiv:1103.1591 [hep-ph]].
- [11] L. Gamberg, Z. -B. Kang and A. Prokudin, Phys. Rev. Lett. **110**, 232301 (2013) [arXiv:1302.3218 [hep-ph]].
- [12] L. Gamberg and Z. -B. Kang, Phys. Lett. B **718** (2012) 181 [arXiv:1208.1962 [hep-ph]]; Phys. Lett. B **696**, 109 (2011) [arXiv:1009.1936 [hep-ph]]; U. D’Alesio, L. Gamberg, Z. -B. Kang, F. Murgia and C. Pisano, Phys. Lett. B **704**, 637 (2011) [arXiv:1108.0827 [hep-ph]].
- [13] Z. -B. Kang and A. Prokudin, Phys. Rev. D **85**, 074008 (2012) [arXiv:1201.5427 [hep-ph]].
- [14] A. Metz, D. Pitonyak, A. Schafer, M. Schlegel, W. Vogelsang and J. Zhou, Phys. Rev. D **86**, 094039 (2012) [arXiv:1209.3138 [hep-ph]].
- [15] D. W. Sivers, Phys. Rev. D **41**, 83 (1990); Phys. Rev. D **43**, 261 (1991).
- [16] Z. -B. Kang and J. -W. Qiu, Phys. Rev. Lett. **103**, 172001 (2009) [arXiv:0903.3629 [hep-ph]].
- [17] A. Airapetian *et al.* [HERMES Collaboration], Phys. Rev. Lett. **103**, 152002 (2009) [arXiv:0906.3918 [hep-ex]].
- [18] M. Alekseev *et al.* [COMPASS Collaboration], Phys. Lett. B **673**, 127 (2009) [arXiv:0802.2160 [hep-ex]].
- [19] C. Adolph *et al.* [COMPASS Collaboration], Phys. Lett. B **717**, 383 (2012) [arXiv:1205.5122 [hep-ex]].
- [20] X. Qian *et al.* [Jefferson Lab Hall A Collaboration], Phys. Rev. Lett. **107**, 072003 (2011) [arXiv:1106.0363 [nucl-ex]].
- [21] COMPASS proposal at CERN,  
[http://wwwcompass.cern.ch/compass/proposal/compass-II\\_proposal/compass-II\\_proposal.pdf](http://wwwcompass.cern.ch/compass/proposal/compass-II_proposal/compass-II_proposal.pdf).
- [22] Fermilab DY proposal - polarized beam,  
[http://www.fnal.gov/directorate/program\\_planning/June2012Public/P-1027\\_Pol-Drell-Yan-proposal.pdf](http://www.fnal.gov/directorate/program_planning/June2012Public/P-1027_Pol-Drell-Yan-proposal.pdf).
- [23] Fermilab DY proposal - polarized target,  
[http://www.fnal.gov/directorate/program\\_planning/June2013PACPublic/P-1039\\_L0I\\_polarized\\_DY.pdf](http://www.fnal.gov/directorate/program_planning/June2013PACPublic/P-1039_L0I_polarized_DY.pdf).
- [24] ANDY proposal, [http://www.bnl.gov/npp/docs/pac0611/DY\\_pro\\_110516\\_final.2.pdf](http://www.bnl.gov/npp/docs/pac0611/DY_pro_110516_final.2.pdf).
- [25] Z. -B. Kang, B. -W. Xiao and F. Yuan, Phys. Rev. Lett. **107**, 152002 (2011) [arXiv:1106.0266 [hep-ph]].
- [26] J. C. Collins, *Foundations of Perturbative QCD* (Cambridge University Press, Cambridge, 2011).
- [27] S. M. Aybat and T. C. Rogers, Phys. Rev. D **83**, 114042 (2011) [arXiv:1101.5057 [hep-ph]].
- [28] S. M. Aybat, J. C. Collins, J. -W. Qiu and T. C. Rogers, Phys. Rev. D **85**, 034043 (2012) [arXiv:1110.6428 [hep-ph]].

- [29] M. G. Echevarria, A. Idilbi, A. Schafer and I. Scimemi, *Eur. Phys. J. C* **73**, 2636 (2013) [arXiv:1208.1281 [hep-ph]].
- [30] P. Sun and F. Yuan, *Phys. Rev. D* **88**, 034016 (2013) [arXiv:1304.5037 [hep-ph]].
- [31] Z. -B. Kang and J. -W. Qiu, *Phys. Rev. D* **79**, 016003 (2009) [arXiv:0811.3101 [hep-ph]].
- [32] J. Zhou, F. Yuan and Z. -T. Liang, *Phys. Rev. D* **79**, 114022 (2009) [arXiv:0812.4484 [hep-ph]].
- [33] W. Vogelsang and F. Yuan, *Phys. Rev. D* **79**, 094010 (2009) [arXiv:0904.0410 [hep-ph]].
- [34] V. M. Braun, A. N. Manashov and B. Pirnay, *Phys. Rev. D* **80**, 114002 (2009) [arXiv:0909.3410 [hep-ph]].
- [35] Z. -B. Kang, *Phys. Rev. D* **83**, 036006 (2011) [arXiv:1012.3419 [hep-ph]].
- [36] A. Schafer and J. Zhou, *Phys. Rev. D* **85**, 117501 (2012) [arXiv:1203.5293 [hep-ph]].
- [37] Z. -B. Kang and J. -W. Qiu, *Phys. Lett. B* **713**, 273 (2012) [arXiv:1205.1019 [hep-ph]]; Z. -B. Kang, I. Vitev and H. Xing, *Phys. Rev. D* **87**, no. 3, 034024 (2013) [arXiv:1212.1221].
- [38] J. P. Ma and Q. Wang, *Phys. Lett. B* **715**, 157 (2012) [arXiv:1205.0611 [hep-ph]].
- [39] J. C. Collins, D. E. Soper and G. F. Sterman, *Nucl. Phys. B* **250**, 199 (1985).
- [40] J. -w. Qiu and X. -f. Zhang, *Phys. Rev. Lett.* **86**, 2724 (2001) [hep-ph/0012058]; *Phys. Rev. D* **63**, 114011 (2001) [hep-ph/0012348].
- [41] F. Landry, R. Brock, P. M. Nadolsky and C. P. Yuan, *Phys. Rev. D* **67**, 073016 (2003) [hep-ph/0212159].
- [42] M. Guzzi, P. M. Nadolsky and B. Wang, arXiv:1309.1393 [hep-ph].
- [43] P. M. Nadolsky, D. R. Stump and C. P. Yuan, *Phys. Rev. D* **64**, 114011 (2001) [hep-ph/0012261].
- [44] C. A. Aidala, B. Field, L. P. Gamberg and T. C. Rogers, arXiv:1401.2654 [hep-ph].
- [45] S. M. Aybat, A. Prokudin and T. C. Rogers, *Phys. Rev. Lett.* **108**, 242003 (2012) [arXiv:1112.4423 [hep-ph]].
- [46] M. Anselmino, M. Boglione and S. Melis, *Phys. Rev. D* **86**, 014028 (2012) [arXiv:1204.1239 [hep-ph]].
- [47] D. Boer, *Nucl. Phys. B* **874**, 217 (2013) [arXiv:1304.5387 [hep-ph]].
- [48] P. Sun and F. Yuan, *Phys. Rev. D* **88**, 114012 (2013) [arXiv:1308.5003 [hep-ph]].
- [49] M. G. Echevarria, A. Idilbi and I. Scimemi, *Phys. Lett. B* **726** (2013) 795 [arXiv:1211.1947 [hep-ph]].
- [50] M. G. Echevarria, A. Idilbi and I. Scimemi, arXiv:1402.0869 [hep-ph].
- [51] A. V. Konychev and P. M. Nadolsky, *Phys. Lett. B* **633**, 710 (2006) [hep-ph/0506225].
- [52] A. Bacchetta, U. D'Alesio, M. Diehl and C. A. Miller, *Phys. Rev. D* **70**, 117504 (2004) [hep-ph/0410050].
- [53] C. T. H. Davies, B. R. Webber and W. J. Stirling, *Nucl. Phys. B* **256**, 413 (1985).
- [54] R. K. Ellis, D. A. Ross and S. Veseli, *Nucl. Phys. B* **503**, 309 (1997) [hep-ph/9704239].
- [55] M. Anselmino, M. Boglione, U. D'Alesio, A. Kotzinian, F. Murgia and A. Prokudin, *Phys. Rev. D* **71**, 074006 (2005) [hep-ph/0501196].
- [56] J. C. Collins, A. V. Efremov, K. Goeke, S. Menzel, A. Metz and P. Schweitzer, *Phys. Rev. D* **73**, 014021 (2006) [hep-ph/0509076].
- [57] P. Schweitzer, T. Teckentrup and A. Metz, *Phys. Rev. D* **81**, 094019 (2010) [arXiv:1003.2190 [hep-ph]].
- [58] Note the more recent analysis in [59] is roughly consistent with our range, while those in [60] on the HERMES data lead to even more freedom on the  $\langle k_{\perp}^2 \rangle_{Q^0}$  and  $\langle p_T^2 \rangle_{Q^0}$ .
- [59] A. Signori, A. Bacchetta, M. Radici and G. Schnell, *JHEP* **1311**, 194 (2013) [arXiv:1309.3507 [hep-ph]].
- [60] M. Anselmino, M. Boglione, J. O. G. H., S. Melis and A. Prokudin, arXiv:1312.6261 [hep-ph].
- [61] Z. -B. Kang and J. -W. Qiu, *Phys. Rev. D* **78**, 034005 (2008) [arXiv:0806.1970 [hep-ph]]; R. -b. Meng, F. I. Olness and D. E. Soper, *Nucl. Phys. B* **371**, 79 (1992); H. Eguchi, Y. Koike and K. Tanaka, *Nucl. Phys. B* **763**, 198 (2007) [hep-ph/0610314].
- [62] M. G. Echevarria, A. Idilbi and I. Scimemi, *JHEP* **1207** (2012) 002 [arXiv:1111.4996 [hep-ph]].
- [63] Z. -B. Kang and J. -W. Qiu, *Phys. Rev. D* **81**, 054020 (2010) [arXiv:0912.1319 [hep-ph]].
- [64] A. D. Martin, W. J. Stirling, R. S. Thorne and G. Watt, *Eur. Phys. J. C* **63**, 189 (2009) [arXiv:0901.0002 [hep-ph]].
- [65] D. de Florian, R. Sassot and M. Stratmann, *Phys. Rev. D* **75**, 114010 (2007) [hep-ph/0703242 [HEP-PH]].
- [66] Z. -B. Kang and J. -W. Qiu, *Phys. Lett. B* **721**, 277 (2013) [arXiv:1212.6541]; Z. -B. Kang, X. Liu and S. Mantry, arXiv:1312.0301 [hep-ph].
- [67] B. Abbott *et al.* [D0 Collaboration], *Phys. Lett. B* **513**, 292 (2001) [hep-ex/0010026].
- [68] B. Abbott *et al.* [D0 Collaboration], *Phys. Rev. D* **61**, 032004 (2000) [hep-ex/9907009].
- [69] T. Affolder *et al.* [CDF Collaboration], *Phys. Rev. Lett.* **84**, 845 (2000) [hep-ex/0001021].
- [70] S. Chatrchyan *et al.* [CMS Collaboration], *Phys. Rev. D* **85**, 032002 (2012) [arXiv:1110.4973 [hep-ex]].
- [71] A. S. Ito, R. J. Fisk, H. Jostlein, D. M. Kaplan, S. W. Herb, D. C. Hom, L. M. Lederman and H. D. Snyder *et al.*, *Phys. Rev. D* **23**, 604 (1981).
- [72] G. Moreno, C. N. Brown, W. E. Cooper, D. Finley, Y. B. Hsiung, A. M. Jonckheere, H. Jostlein and D. M. Kaplan *et al.*, *Phys. Rev. D* **43**, 2815 (1991).
- [73] K. J. Eskola, V. J. Kolhinen and C. A. Salgado, *Eur. Phys. J. C* **9**, 61 (1999) [hep-ph/9807297].
- [74] C. Adolph *et al.* [COMPASS Collaboration], *Eur. Phys. J. C* **73**, 2531 (2013) [arXiv:1305.7317 [hep-ex]].
- [75] A. Airapetian *et al.* [HERMES Collaboration], *Phys. Rev. D* **87**, 074029 (2013) [arXiv:1212.5407 [hep-ex]].
- [76] U. D'Alesio, M. G. Echevarria, A. Idilbi, S. Melis, I. Scimemi, *in preparation*.
- [77] A. Bacchetta, M. Diehl, K. Goeke, A. Metz, P. J. Mulders and M. Schlegel, *JHEP* **0702**, 093 (2007) [hep-ph/0611265].
- [78] M. Anselmino, M. Boglione, U. D'Alesio, A. Kotzinian, S. Melis, F. Murgia, A. Prokudin and C. Turk, *Eur. Phys. J. A* **39**, 89 (2009) [arXiv:0805.2677 [hep-ph]].
- [79] C. Kouvaris, J. -W. Qiu, W. Vogelsang and F. Yuan, *Phys. Rev. D* **74**, 114013 (2006) [hep-ph/0609238].
- [80] A. Bacchetta and M. Radici, *Phys. Rev. Lett.* **107**, 212001 (2011) [arXiv:1107.5755 [hep-ph]].



- [81] J. C. Collins, A. V. Efremov, K. Goetze, M. Grosse Perdekamp, S. Menzel, B. Meredith, A. Metz and P. Schweitzer, Phys. Rev. D **73**, 094023 (2006) [hep-ph/0511272].
- [82] W. Vogelsang and F. Yuan, Phys. Rev. D **72**, 054028 (2005) [hep-ph/0507266].
- [83] M. Anselmino, M. Boglione, U. D'Alesio, S. Melis, F. Murgia and A. Prokudin, Phys. Rev. D **79**, 054010 (2009) [arXiv:0901.3078 [hep-ph]].
- [84] Z. -B. Kang and B. -W. Xiao, Phys. Rev. D **87**, 034038 (2013) [arXiv:1212.4809 [hep-ph]].
- [85] M. Anselmino, M. Boglione, U. D'Alesio, S. Melis, F. Murgia and A. Prokudin, Phys. Rev. D **81**, 034007 (2010) [arXiv:0911.1744 [hep-ph]]; Z. -B. Kang, A. Metz, J. -W. Qiu and J. Zhou, Phys. Rev. D **84**, 034046 (2011) [arXiv:1106.3514 [hep-ph]]; A. Adare *et al.* [PHENIX Collaboration], arXiv:1312.1995 [hep-ex]; K. Allada *et al.* [Jefferson Lab Hall A Collaboration], arXiv:1311.1866 [nucl-ex]; J. Adams *et al.* [STAR Collaboration], Phys. Rev. Lett. **92**, 171801 (2004) [hep-ex/0310058].
- [86] P. J. Sutton, A. D. Martin, R. G. Roberts and W. J. Stirling, Phys. Rev. D **45**, 2349 (1992).